Journal Pre-proof

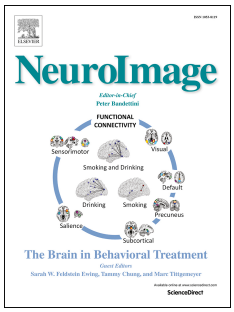

Combining fMRI during resting state and an attention bias task in children

Anita Harrewijn, Rany Abend, Julia Linke, Melissa A. Brotman, Nathan A. Fox, Ellen Leibenluft, Anderson M. Winkler, Daniel S. Pine

PII: S1053-8119(19)30892-4

DOI: https://doi.org/10.1016/j.neuroimage.2019.116301

Reference: YNIMG 116301

To appear in: *NeuroImage*

Received Date: 8 August 2019

Revised Date: 1 October 2019

Accepted Date: 17 October 2019

Please cite this article as: Harrewijn, A., Abend, R., Linke, J., Brotman, M.A., Fox, N.A., Leibenluft, E., Winkler, A.M., Pine, D.S., Combining fMRI during resting state and an attention bias task in children, *NeuroImage* (2019), doi: https://doi.org/10.1016/j.neuroimage.2019.116301.

This is a PDF file of an article that has undergone enhancements after acceptance, such as the addition of a cover page and metadata, and formatting for readability, but it is not yet the definitive version of record. This version will undergo additional copyediting, typesetting and review before it is published in its final form, but we are providing this version to give early visibility of the article. Please note that, during the production process, errors may be discovered which could affect the content, and all legal disclaimers that apply to the journal pertain.

© 2019 Published by Elsevier Inc.

Journal Pre-proof

Combining fMRI during resting state and an attention bias task in children

Anita Harrewijn[1], Rany Abend[1], Julia Linke[1], Melissa A. Brotman[1], Nathan A. Fox[2], Ellen Leibenluft[1], Anderson M. Winkler[1], & Daniel S. Pine[1]

1. Emotion and Development Branch, National Institute of Mental Health, 9000 Rockville Pike, Bethesda, MD, 20892, USA

2. Department of Human Development and Quantitative Methodology, University of Maryland, 3304 Benjamin Building, College Park, MD, 20742-1131, USA

Journal Pre-proof

Corresponding author:

Anita Harrewijn, PhD

anitaharrewijn@gmail.com

9000 Rockville Pike

North Drive building 15K

Bethesda, Maryland, 20892

+1 301 827 1871

Journal Pre-proof

Abstract

Neuroimaging studies typically focus on either resting state or task-based fMRI data. Prior research has shown that similarity in functional connectivity between rest and cognitive tasks, interpreted as reconfiguration efficiency, is related to task performance and IQ. Here, we extend this approach from adults to children, and from cognitive tasks to a threat-based attention task. The goal of the current study was to examine whether similarity in functional connectivity during rest and an attention bias task relates to threat bias, IQ, anxiety symptoms, and social reticence. fMRI was measured during resting state and during the dot-probe task in 41 children (M = 13.44, SD = 0.70). Functional connectivity during rest and dot-probe was positively correlated, suggesting that functional hierarchies in the brain are stable. Similarity in functional connectivity between rest and the dot-probe task only related to threat bias ($p_{uncorr} < .03$). This effect did not survive correction for multiple testing. Overall, children who allocate more attention towards threat also may possess greater reconfiguration efficiency in switching from intrinsic to threat-related attention states. Finally, functional connectivity correlated negatively across the two conditions of the dot-probe task. Opposing patterns of modulation of functional connectivity by threat-congruent and threat-incongruent trials may reflect task-specific network changes during two different attentional processes.

Journal Pre-proof

Keywords: attention bias, functional connectivity, fMRI, resting state

Journal Pre-proof

Journal Pre-proof

1. Introduction

Neuroimaging studies typically focus on either resting state or task-based fMRI[1] data. Recent studies have combined resting state and task-related fMRI data to gain insights on the relation between brain function and behavior (Bolt, Nomi, Rubinov, & Uddin, 2017; J. R. Cohen & D'Esposito, 2016; Hearne, Cocchi, Zalesky, & Mattingley, 2017; Ito et al., 2017; Mennes et al., 2010; Schultz & Cole, 2016). One approach of combining these two types of data is to investigate the similarity in functional connectivity between resting state and task data (Schultz & Cole, 2016). The current study extends this approach from adults to children, and from cognitive tasks to a threat-based attention task. This is important to test whether this novel analytic approach can be used in the field of developmental psychopathology.

Resting-state functional connectivity refers to temporal correlations that index brain network intrinsic activity (Fox & Raichle, 2007). Functional connectivity during rest and cognitive tasks appear to be strongly related, suggesting the presence of stable functional hierarchies (Smith et al., 2009) that reflect both intrinsic, task-general, and also task-specific brain networks (Cole, Bassett, Power, Braver, & Petersen, 2014). Changes in patterns of functional connectivity from intrinsic to task-related states may reflect *reconfiguration efficiency* and can be measured as the similarity in (or correlation between) functional connectivity during rest and task (Schultz & Cole, 2016). When assessed during cognitive tasks, such reconfiguration efficiency relates to better task performance and, more generally, higher IQ (Schultz & Cole, 2016). We aimed to examine reconfiguration efficiency from rest to task in children, using a paradigm that has successfully uncovered correlates of anxiety, particularly among youth. The

[1] Abbreviations: fMRI = functional magnetic resonance imaging; IQ = intelligence quotient; SCARED = Screen for Child Anxiety Related Disorders; RT = reaction time; ABV = attention bias variability; ICA = independent component analysis; PPI = psychophysiological interaction

study of the reconfiguration efficiency of the emotional attention network around the mean age of onset of several anxiety disorders (e.g., specific phobia, social anxiety disorder) (de Lijster et al., 2017) might yield several new insights into the pathophysiological mechanisms of anxiety disorders.

The dot-probe task examines the effects of threats on attention orienting (Bar-Haim, Lamy, Pergamin, Bakermans-Kranenburg, & van IJzendoorn, 2007). In this task, participants initially view two adjacent faces (angry-neutral, happy-neutral, or neutral-neutral) and then identify the location of a probe replacing either the angry (threat congruent) or neutral (threat incongruent) face (Macleod, Mathews, & Tata, 1986). Meta-analysis relates performance on this task, as expressed in an attention bias towards threats, to anxiety (Bar-Haim et al., 2007). Specifically, higher levels of anxiety predict shorter reaction-times during threat-congruent relative to threat-incongruent trials (threat bias; (Abend et al., 2018; Bar-Haim et al., 2007)).

Several studies have used the dot-probe task in the MRI scanner to investigate mechanisms underlying threat-related attentional processes in youth, focusing on amygdala-related functional connectivity using a seed-based approach. Functional connectivity between the amygdala and several regions during threat-incongruent versus threat-congruent trials has demonstrated stability in youth when measured approximately nine weeks apart (White et al., 2016). Negative functional connectivity between the amygdala and the insula during threat versus neutral trials placed individuals with early-childhood behavioral inhibition at risk for developing internalizing symptoms in adulthood (Hardee et al., 2013). Longitudinal studies found that amygdala-PFC connectivity during threat-congruent moderated relations between early-childhood behavioral inhibition and anxiety symptoms in adolescence (Abend et al., 2019). Moreover, patterns of threat-related amygdala-insula functional connectivity during threat-

congruent trials were found to differentiate pediatric anxiety patients from healthy controls (White et al., 2017).

Of note, prior studies have all used a seed-based approach to study amygdala connectivity during the dot-probe task. Several limitations of this literature are noted. These studies focus on different conditions within the dot-probe task (e.g. threat-incongruent versus threat-congruent). Furthermore, because the amygdala is only one of many regions implicated in anxiety and threat processing (Bruhl, Delsignore, Komossa, & Weidt, 2014; Etkin & Wager, 2007; Xu et al., 2019), whole-network based analyses complement prior studies focused on isolated brain regions. Seed-based connectivity analyses in specific contrasts could be insensitive to network-level perturbations in connectivity, both quantified during resting state and during task-based fMRI. Therefore, it is important to examine functional connectivity on a whole-brain level both at rest and during threat-processing tasks to quantify the neural correlates of anxiety and threat processing. To do so, we extend prior seed-based connectivity findings by examining functional connectivity at the whole brain level, by focusing on reconfiguration efficiency from resting state to the dot-probe task.

Finally, beyond extending previous approaches to emotional-task data in children, the current study also implements two novel procedures to extend previous approaches. First, the study utilizes ICA with both resting-state and task-based data. Second, prior functional connectivity analyses with the dot-probe task used a seed-based approach to contrast connectivity in threat-congruent and threat-incongruent conditions. Beyond comparing connectivity across rest and task, the current study also employs a PPI approach within the emotional task to study modulation of functional connectivity by the two threat-related task conditions.

Journal Pre-proof

The current study assessed similarity in patterns of functional connectivity during rest and the dot-probe task in 13-year-old children, testing five specific hypotheses. First, we hypothesized that functional connectivity during rest correlates strongly with functional connectivity during the dot-probe task (Cole et al., 2014; Schultz & Cole, 2016). Second, we hypothesized that the degree of similarity in functional connectivity between rest and the dot-probe task (i.e., reconfiguration efficiency) relates to task performance (i.e., threat bias) (Schultz & Cole, 2016). Third, we hypothesized that reconfiguration efficiency also relates to IQ. This is because prior work finds IQ to relate to many individual-difference factors among children and adolescents, including performance in many cognitive tasks and many aspects of psychological function. Thus, IQ may also relate to efficiency in switching from resting state to task states in general, both for emotional tasks examined in the current study as well as cognitive tasks more closely linked to IQ in prior work (Schultz & Cole, 2016). Fourth, we hypothesized that reconfiguration efficiency relates to individual differences in anxiety-related measures, such as self-reported and parent-reported anxiety symptoms and socially reticent behavior. Finally, we explored whether task-evoked activity modulates functional connectivity and hypothesized that patterns of connectivity differ between the threat-congruent and threat-incongruent trials of the dot-probe task.

2. Materials and Methods

2.1 Participants

Participants were recruited from a longitudinal study on behaviorally inhibited temperament and early childhood reticence. Data in the current report were collected when the children were approximately 13 years old. 42 children had fMRI data for both resting state and the dot-probe

task. However, for one child, data were excluded because of excessive motion, yielding a final sample of 41 children (19 girls) with a mean age of 13.44 years (*SD* = 0.70, range = 12.42-15.33). Resting state and task-based data were collected on the same day for 25 children, and on different days for 16 children (resting state scan was 1-307 days after the dot-probe scan, median = 101 days). Children entered the longitudinal study through two paths: one group (*n* = 291) was selected based on temperamental reactivity at four months (Hane, Fox, Henderson, & Marshall, 2008) and the other group (*n* = 384) was randomly recruited from the community at age two years (Jarcho et al., 2016; Michalska et al., 2019). Among the 41 children in the current report, 18 were recruited as infants and 23 were recruited at two years. All children provided written assent, and all parents provided written informed consent. The study was approved by the University of Maryland-College Park and National Institute of Mental Health institutional review boards.

Descriptive statistics appear in Table 1. Girls reported slightly more anxiety symptoms than boys, $F(1,39) = 3.85$, $p = 0.057$, but there were no differences between boys and girls on any of the other variables, Fs < 2.91, ps > 0.096. Children selected as infants (*M* = 13.04, *SD* = 0.63) were slightly younger than children recruited at two years (*M* = 13.75, *SD* = 0.61), $F(1,39) = 13.55$, $p = 0.001$. Children who did both scans on the same day (*M* = 13.64, *SD* = 0.65) were slightly older than children who did the scans on different days (*M* = 13.14, *SD* = 0.69), $F(1,39) = 5.49$, $p = 0.024$. No other variables differed between children recruited as infants or at two years or between children who did both scans on same or different days, Fs < 3.20, ps > 0.082. The main analyses were corrected for age, sex, participant recruitment source (i.e., during infancy or at age two years), and time between scans.

Table 1.

Means, standard deviations and range for the behavioral and motion measures across the sample.

	Mean	SD	Min	Max
Age	13.44	0.7	12.42	15.33
Accuracy dot-probe	92.76	4.81	79.8	100
Threat bias	0.81	30.74	-55.89	69.72
Threat ABV	0.05	0.02	0.02	0.1
Happy bias	1.67	25	-66.72	45.32
Happy ABV	0.05	0.03	0.02	0.14
IQ	115.95	13.54	84	140
SCARED-C Total	11.54	7.71	0	32
SCARED-P Total	6.69	6.75	0	31
Social Reticence	-0.02	0.5	-0.99	1.33
std DVARS (task)	1.14	0.05	1.02	1.24
std DVARS (rest)	1.11	0.08	0.95	1.32
DVARS (task)	22.45	3.87	15.71	31.04
DVARS (rest)	21.80	6.72	13.95	40.46
FD (task)	0.12	0.08	0.04	0.38
FD (rest)	0.18	0.14	0.05	0.65

Note: social reticence scores for two participants were missing.

SD = standard deviation; ABV = attention bias variability; SCARED = Screen for Child Anxiety Related Disorders; C = child-reported; P = parent-reported; std DVARS = standardized spatial standard deviation of the data after temporal differencing; DVARS = original spatial standard deviation of the data after temporal differencing; FD = framewise displacements. See main text for definitions of bias and bias variability.

2.2 Dot-probe task

The dot-probe task has been used extensively to measure attention bias to threat (Abend et al., 2019; Bar-Haim et al., 2007; Macleod et al., 1986). In each trial of this task, a pair of faces was shown (either angry-neutral, happy-neutral, or neutral-neutral; see Figure 1). After 500 ms, an arrow (i.e., probe) appeared at the location of one of these faces. The locations of the faces and

arrows were counterbalanced across the task. Participants had to press a button as quickly as possible to indicate the direction of the arrow. In congruent trials the probe was presented at the location of the emotional face, in incongruent trials the probe was presented at the location of the neutral face. The task consisted of 48 threat-congruent, 48 threat-incongruent, 48 happy-congruent, 48 happy-incongruent, and 96 neutral-neutral trials across four blocks of 4:15 minutes. The task was programmed and administered with E-Prime (Psychology Software Tools, Pittsburgh, PA) and faces from the NimStim set were used (Tottenham et al., 2009).

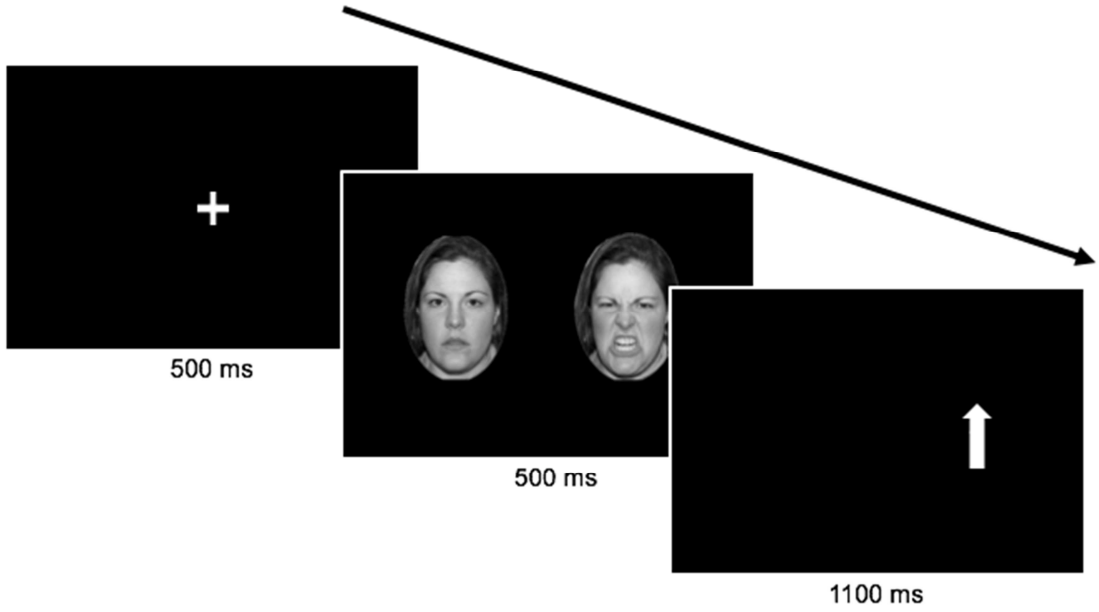

Figure 1. Overview of the dot-probe task.

2.3 Other behavioral measures

2.3.1 IQ. IQ was estimated when children were approximately 10 years old using the vocabulary and matrix reasoning subscales of the Wechsler Abbreviated Scale of Intelligence (Wechsler, 1999). IQ has been shown to have high long-term stability (Canivez & Watkins, 1998; Watkins & Smith, 2013).

2.3.2 Anxiety symptoms. Trait anxiety symptoms were measured using the SCARED, a reliable child- and parent-report questionnaire with 42 items (Birmaher et al., 1997; Muris, Dreessen, Bogels, Weckx, & van Melick, 2004). We used the SCARED total score for self-report and parent-report separately, replacing up to two missing responses in the total score with the subject's mean value for the other items. Children and parents filled out the questionnaire separately within a year of the dot-probe scan (*M*=99.92 days, *SD*=108.29, range = -1 to 348 days), with 31 (75.6%) children and parents completing the SCARED within 6 months. Test-retest reliability of the child- and parent-reported SCARED total score is moderate to good over a period of three to six months (Behrens, Swetlitz, Pine, & Pagliaccio, 2019; Birmaher et al., 1997; Boyd, Ginsburg, Lambert, Cooley, & Campbell, 2003; Haley, Puskar, & Terhorst, 2011). Over a period of five years, most anxiety symptoms slightly decrease, whereas social anxiety symptoms remain relatively stable and generalized anxiety symptoms slightly increase in adolescent girls (Hale, Raaijmakers, Muris, van Hoof, & Meeus, 2008).

2.3.3 Social reticence. Social reticence reflects shy and anxiously avoidant behavior during early childhood (Degnan et al., 2014), and predicts later anxiety symptoms and related neural measures (Jarcho et al., 2016; Michalska et al., 2019). It was measured using a composite score of maternal-report questionnaires and behavioral observations collected at 2, 3, 4, 5, and 7 years of age (Jarcho et al., 2016; Michalska et al., 2019). The Social Fear subscale from the Toddler Behavioral Assessment Questionnaire (Goldsmith, 1996) was used at 2 and 3 years, and the Shyness subscale from the Children's Behavior Questionnaire (Rothbart, Ahadi, Hershey, & Fisher, 2001) was used at 4, 5 and 7 years. Socially reticent behavior was observed during free play, cleanup and social problem-solving interactions with an unfamiliar, age-matched peer at 2,

3, 4, 5 and 7 years (Degnan et al., 2014; Degnan et al., 2011). All subscales and behavior scores were standardized within timepoint and averaged together.

2.4 fMRI data collection

fMRI data were collected during resting state and the dot-probe task on a 3T MR750 General Electric scanner (Waukesha, Wisconsin, USA) with a 32-channel head coil. For resting state, 180 functional image volumes with 47 contiguous interleaved axial slices were collected with a T2*-weighted echo-planar sequence (TR = 2000ms, TE = 30ms, flip angle = 90, field of view (FOV) = 192mm, matrix = 64x64, in plane resolution 3x3x4mm). For each of the four blocks of the dot-probe task, 111 functional image volumes with 47 contiguous interleaved axial slices were collected with a T2*-weighted echo-planar sequence (TR = 2300ms, TE = 25ms, flip angle = 50, FOV = 240mm, matrix = 96×96 in plane resolution 2.5×2.5×3mm). In addition, a high-resolution T1-weighted whole-brain volumetric scan was acquired during each scan session, with a high-resolution magnetization prepared gradient echo sequence (MPRAGE; TE = min full; TI = 425ms; flip angle = 7; FOV = 256mm; matrix = 256×256; in plane resolution = 1x1x1mm).

2.5 Behavioral analysis

Selection of dot-probe trials to be included in analyses followed the same criteria used by Abend et al. (2019). Trials were included only if the response to the probe was correct and if RT was between 150 and 2000 ms and less than 2.5 standard deviations away from the participant's mean RT. In line with prior studies (Abend et al., 2019; White et al., 2017), task data were considered valid if accuracy was ≥70%; all 41 participants surpassed this threshold. Task performance was measured by calculating threat bias scores (mean RT in threat-incongruent

trials minus mean RT in threat-congruent trials), with higher scores reflecting an attention bias towards threat (that is, slower responding in threat-incongruent trials). Happy bias scores were also calculated (mean RT in happy-incongruent minus mean RT in happy-congruent trials).

In addition, secondary analyses examined ABV, an index of temporal variability in attention allocation previously found to relate to anxiety symptoms and brain function (Abend et al., 2019; Iacoviello et al., 2014). In a moving-window analysis, threat bias scores (as described above) were calculated for all 10 successive angry-neutral trials. The standard deviation of all these threat bias scores within one participant was calculated, and then divided by the overall mean RT of the participant. The procedure was repeated for happy-neutral trials to calculate happy ABV scores (Abend et al., 2019).

2.6 fMRI preprocessing

Quality of fMRI data was assessed using the MRI Quality Control tool (MRIQC) (Esteban et al., 2017). Data of one participant were excluded, because this subject was an outlier based on AFNI's outlier ratio and because visual inspection showed excessive movement. The first 4 TRs from each scan were removed to account for non-steady-state data. fMRI data from resting state and the dot-probe task were preprocessed using fMRIPrep (Esteban et al., 2019) including the following steps: skull stripping, correction for head-motion parameters, slice time correction, co-registration to corresponding structural image (boundary-based registration with 9 degrees of freedom), spatial normalization to MNI space (nonlinear registration), and ICA-AROMA (Pruim et al., 2015). All spatial transformations in fMRIPrep are done in one step, to allow for a single-interpolation resampling of volumes.

Journal Pre-proof

Journal Pre-proof

The following nuisance variables were regressed out from both resting state and dot-probe time series: motion parameters (translation in x, y and z directions, plus rotations around these axes), cerebral spinal fluid signal, white matter signal, original and standardized spatial standard deviation of the data after temporal differencing (DVARS and std DVARS), framewise displacement (Power, Barnes, Snyder, Schlaggar, & Petersen, 2012), 6 temporal and anatomical noise components calculated with CompCor (Behzadi, Restom, Liau, & Liu, 2007), cosine variables, and ICA-AROMA components that were classified as related to head motion. The data for both rest and task were high-pass filtered (0.04 Hz). Correlations between motion variables and the behavioral variables are shown in Table 2.

Table 2.

Pearson's correlations between motion, behavioral and neural variables.

	std DVARS (task)	std DVARS (rest)	DVARS (task)	DVARS (rest)	FD (task)	FD (rest)
Age	-0.03	-0.02	0.01	0.09	0.05	0.17
Accuracy dot-probe	0.04	0.04	-0.05	0.05	-0.06	0.12
Threat bias	0.10	0.01	-0.07	-0.14	-0.15	-0.22
Threat ABV	0.10	-0.24	0.08	0.10	0.02	0.10
Happy bias	0.02	-0.17	0.06	0.24	0.16	0.30
Happy ABV	0.22	-0.27	0.24	0.19	0.16	0.12
IQ	0.15	-0.20	0.02	-0.09	0.00	-0.06
SCARED-C Total	-0.33*	-0.03	-0.29	-0.11	-0.14	-0.06
SCARED-P Total	0.14	0.10	0.00	-0.12	-0.10	-0.18
Social Reticence	0.10	0.15	-0.12	-0.09	-0.14	-0.09
Similarity	0.11	0.09	-0.23	-0.29	-0.27	-0.25
Distance	0.12	0.02	-0.11	-0.34*	-0.12	-0.30
Similarity PPI	-0.03	0.09	0.18	0.30	0.10	0.19
Distance PPI	0.06	0.31*	-0.10	0.07	-0.23	-0.09

Note: * $p < 0.05$, uncorrected.

Journal Pre-proof

ABV = attention bias variability; SCARED = Screen for Child Anxiety Related Disorders; C = child-reported; P = parent-reported; std DVARS = standardized spatial standard deviation of the data after temporal differencing; DVARS = original spatial standard deviation of the data after temporal differencing; FD = framewise displacements.

2.7 ICA and dual regression

ICA was run on the resting state data using Multivariate Exploratory Linear Optimized Decomposition into Independent Components (MELODIC). The model order was selected using Bayesian methods described in Beckmann and Smith (2004); 20 components were automatically identified. After visual inspection, three were removed as they were comprised of regions occupied by cerebrospinal fluid or other non-brain tissue. The remaining 17 components were selected for further analyses (Figure 2). Naming of these components was based on putative functions related to their topography; we also used previous literature on resting-state imaging as reference (Beckmann, DeLuca, Devlin, & Smith, 2005; Damoiseaux et al., 2006; Smith et al., 2009). Time series for these 17 components were extracted from resting state and from dot-probe data (in native resolution) using dual regression in FSL (Filippini et al., 2009). Thus, for each independent component, a time course for rest and another for the dot-probe task were obtained. In addition, for the dot-probe task, task events (threat-congruent, threat-incongruent, happy-congruent, happy-incongruent, and neutral trials and trials with errors) were convolved using a canonical hemodynamic response function (HRF) approach with Glover's HRF (Glover, 1999) and were regressed out from the fMRI time course.

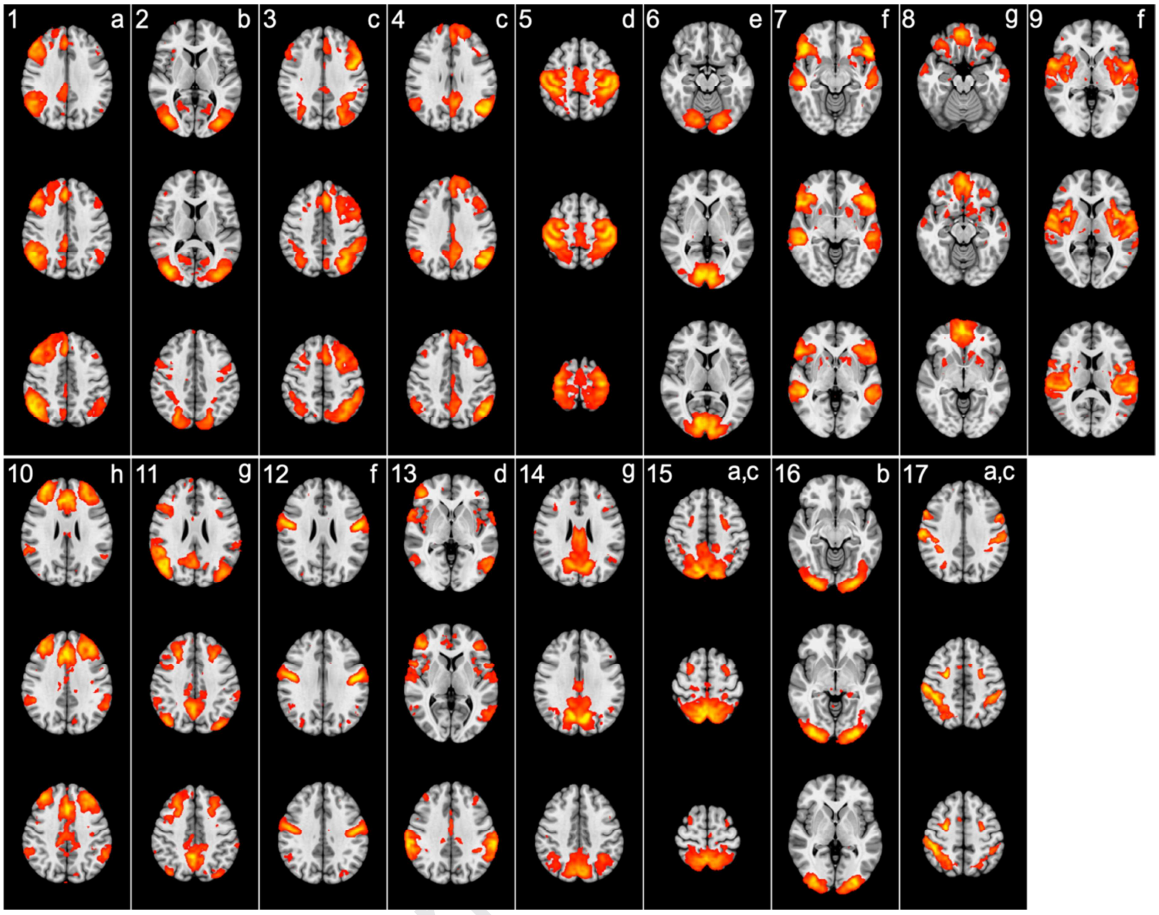

Figure 2. Spatial maps for each of the 17 independent components. Their putative functional interpretation based on previous studies is as follows: a = right dorsal visual stream, b = lateral visual cortical areas, c = left dorsal visual stream, d = sensory-motor system, e = medial visual cortical areas, f = auditory system, g = visuo-spatial system, h = executive control.

2.8 Functional connectivity and clustering

Full and partial correlations between each pair of the 17 components were calculated as measurements of functional connectivity, converted to a z-score using Fisher's r-to-z transformation, and assembled into connectivity matrices. For each subject, this generated one functional connectivity matrix for resting state and another for the dot-probe task. Since these

Journal Pre-proof

matrices are symmetric, for convenience we chose to retain only the upper triangular part (above the main diagonal) for partial correlations, leaving the lower triangular part (below the main diagonal) to hold the full (not partial) correlations, thus avoiding redundancies when generating figures. These steps were conducted using customized FSLNets scripts (http://fsl.fmrib.ox.ac.uk/fsl/fslwiki/FSLNets) (Smith et al., 2013). To assess the similarity between these two matrices, the partial correlations above the main diagonal of each matrix were unwrapped into a vector, and the Pearson's correlation between the vector for resting state and the vector for the dot-probe task was calculated and converted to a z-score using Fisher's r-to-z transformation (Schultz & Cole, 2016)[2]. These steps were performed for each participant, thereby generating one similarity value for each participant.

For visualization purposes, functional connectivity matrices were averaged across participants. To visualize the temporal proximity between the 17 ICA components, these components were clustered using hierarchical nearest neighbor with Ward's linkage as implemented in FSLNets.

To investigate whether task-evoked activity would modulate functional connectivity, two additional functional connectivity matrices, one for the threat-congruent and another for the threat-incongruent trials, were computed using a PPI strategy (Friston et al., 1997; O'Reilly, Woolrich, Behrens, Smith, & Johansen-Berg, 2012). Instead of computing the correlation in the time series between all 17 components (FC), we performed a regression analysis with the time series of one component modulated by the time series for threat-congruent trials (i.e., an interaction term) predicting the time series of another component, while including the modeled time series for threat-congruent trials as nuisance. This analysis assessed whether functional

[2] Note that at this stage, investigations that use both resting state and task-based fMRI do not require these two modalities have the same spatial or temporal resolution.

connectivity between these two components would be modulated by threat-congruent trials. This was done for all 17 components predicting all other components, resulting in a matrix similar to the FC matrix. As with the analyses for rest and task data, Pearson's correlation between these two matrices for each participant were calculated, and then subjected to the Fisher's r-to-z-transformation.

2.9 Between-subject statistical analysis

Group analyses assessed whether similarity in functional connectivity during rest and dot-probe was related to task performance (threat bias) as well as IQ, anxiety symptoms, and social reticence. These analyses used nonparametric permutation inference using Permutation Analysis of Linear Models (PALM) (Winkler, Ridgway, Webster, Smith, & Nichols, 2014). Five designs were tested, each including similarity as the dependent variable, an intercept, nuisance variables, and an independent variable of interest (Table 2) Only the independent variable of interest differed per design, such that each design tested how the similarity in functional connectivity during rest and dot-probe relates to threat bias, IQ, child-reported anxiety symptoms, parent-reported anxiety symptoms, and social reticence. We tested both positive and negative effects (i.e., contrasts) for each of these five independent variables of interest, e.g. a positive effect of threat bias on similarity and a negative effect of threat bias on similarity in design 1. For the first design (testing threat bias), we also tested the intercept, that is, whether the correlation between resting state and dot-probe functional connectivity matrices was significantly different than zero. Family-wise error rate (FWER) was used in PALM to correct non-parametrically for multiple testing across the five designs (Winkler et al., 2016).

Journal Pre-proof

Journal Pre-proof

Table 3.

Overview of the five designs that were tested using nonparametric permutation tests.

	Design 1	Design 2	Design 3	Design 4	Design 5
Dependent variable	Similarity	Similarity	Similarity	Similarity	Similarity
Independent variable of interest	Threat bias	IQ	SCARED-C Total	SCARED-P Total	Social Reticence
Nuisance variables	Age	Age	Age	Age	Age
	Sex	Sex	Sex	Sex	Sex
	Participant recruitment source	Participant recruitment source	Participant recruitment source	Participant recruitment source	Participant recruitment source
	Time between scans	Time between scans	Time between scans	Time between scans	Time between scans
	Intercept	Intercept	Intercept	Intercept	Intercept

Note: SCARED = Screen for Child Anxiety Related Disorders; C = child-reported; P = parent-reported

A final set of exploratory nonparametric permutation tests in PALM was performed on six different dependent variables: similarity, distance measures (correlations between two vectors transformed to Euclidean distances), functional connectivity matrix during rest (full and partial correlations), and functional connectivity matrix during task (full and partial correlations). Consistent with the previous five designs, these analyses included each an intercept and the following nuisance variables: age, sex, participant recruitment source (i.e., during infancy or at age two years), and time between scans. We tested twelve different designs, each with the nuisance variables and one extra independent variable of interest: threat bias, IQ, child-reported anxiety symptoms, parent-reported anxiety symptoms, social reticence, interaction between sex and child-reported anxiety symptoms, interaction between sex and parent-reported anxiety

Journal Pre-proof

symptoms, absolute threat bias, threat ABV, happy bias, absolute happy bias, and happy ABV (Supplementary Table 1). The p-values were corrected non-parametrically for multiple testing across the six independent variables and twelve designs in PALM using FWER (Winkler et al., 2016). The main analysis with five designs and the exploratory analyses with twelve designs were repeated for the functional connectivity matrices based on PPI analysis.

3. Results

3.1 Functional connectivity matrices

Three clusters of correlated networks emerged from the data in both resting state and dot-probe functional connectivity matrices: one cluster encompassing default-mode, executive control, visual, and auditory networks; a second encompassing visual networks; and a third encompassing sensory-motor and auditory networks (see Figure 3 and 4 for the FC matrices with z-statistics, and see Supplementary Figures 1 and 2 for the FC matrices with *r*s). The cluster encompassing sensory-motor and auditory networks was the same during resting state and the dot-probe task. The only difference in clustering between the resting state and the dot-probe task was that two networks (left dorsal visual stream [component 3] and left/right dorsal visual stream [component 15]) were part of the visual cluster during resting state and part of the default-mode, executive control, visual and auditory cluster during the dot-probe task[3]. Treated separately, patterns of correlations during either resting state or the dot-probe task were unrelated to threat bias, IQ, anxiety symptoms, social reticence or any other measures from secondary regression analyses.

[3] We reran the same analysis stream for examining the similarity between resting state and the dot-probe task without component 3 and 15, to investigate whether the association with threat bias would be stronger if only the stable networks were considered. The results, however, remained the same.

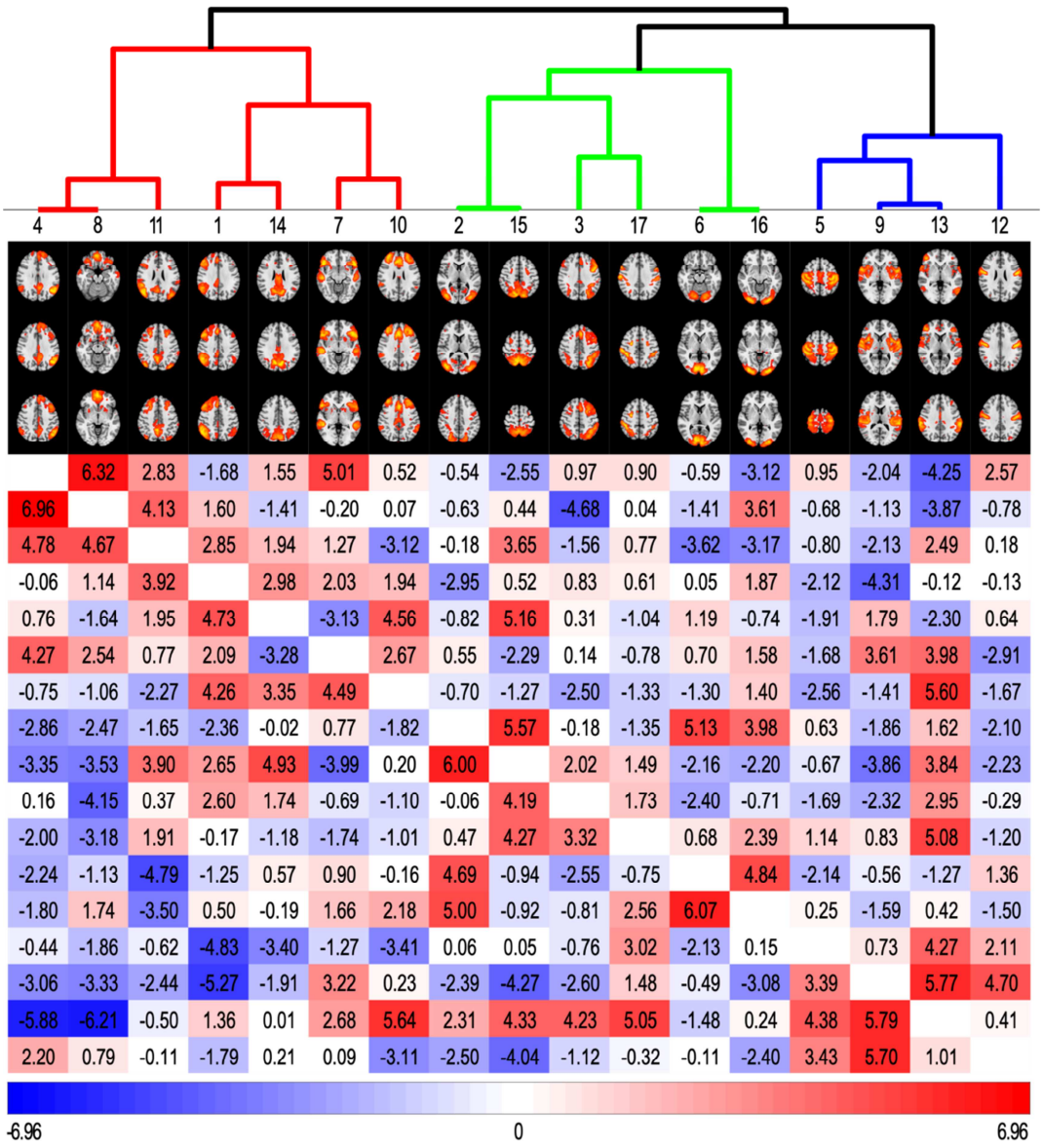

Figure 3. Functional connectivity matrix during resting state. Full correlations (transformed to z-statistics) are presented below the diagonal, partial correlations (transformed to z-statistics) are presented above the diagonal. Three clusters emerged: a) visuo-spatial system, executive control and some visual and auditory networks (in red); b) visual networks (in green); and c) sensory-motor and auditory networks (in blue). Components with more similar time courses appear closer together. The threshold for unique colors in the dendrogram was set at 0.75.

Note: numbers correspond to the 17 components from Figure 2.

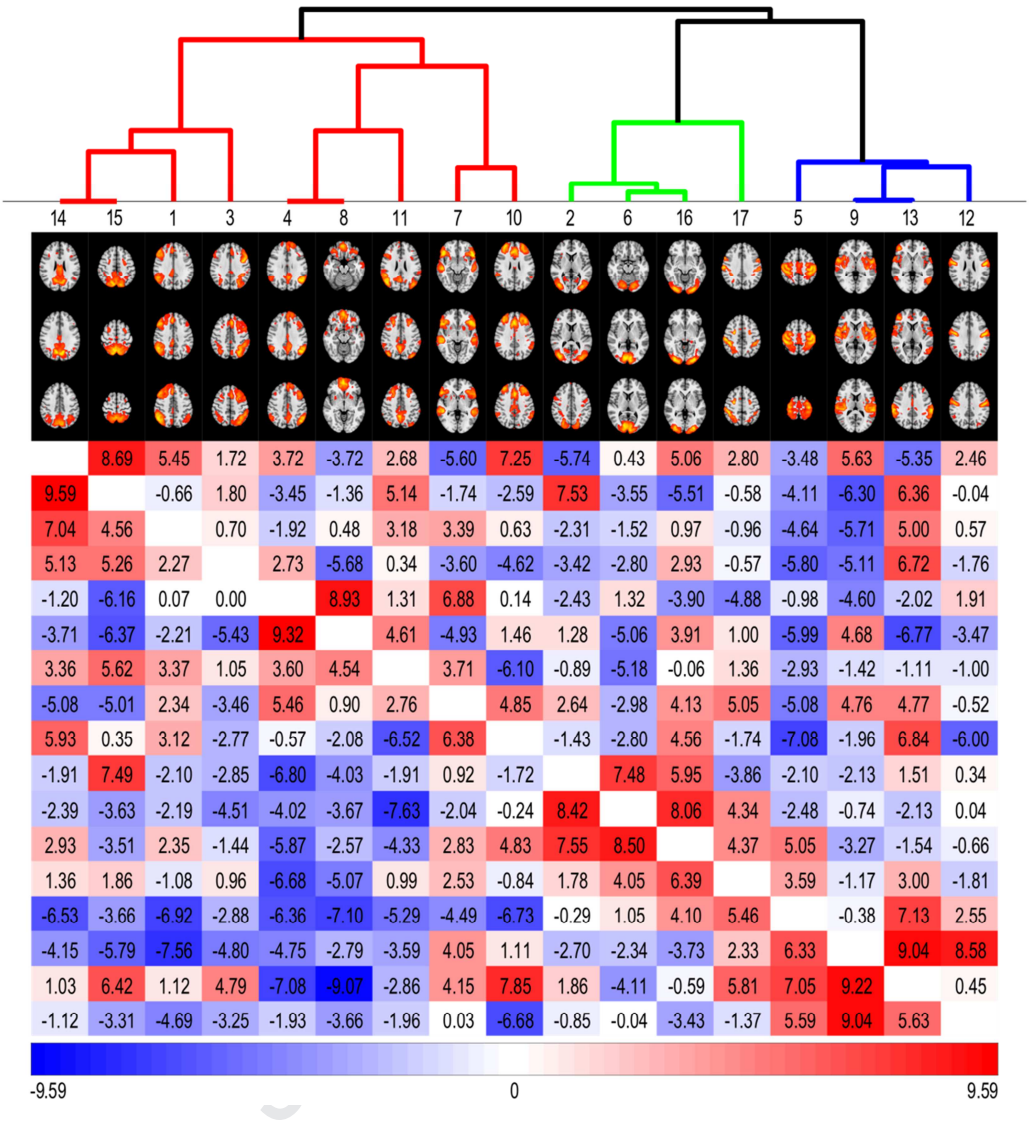

Figure 4. Functional connectivity matrix during the dot-probe task. Full correlations (transformed to z-statistics) are presented below the diagonal, partial correlations (transformed to z-statistics) are presented above the diagonal. Three clusters emerged: a) visuo-spatial system, executive control and some visual and auditory networks (in red); b) visual networks (in green); and c) sensory-motor and auditory networks (in blue). Components with more similar time courses appear closer together. The threshold for unique colors in the dendrogram was set at 0.75.

Note: numbers correspond to the 17 components (based on resting state data) from Figure 2.

3.2 Similarity between resting state and the dot-probe task

The first PALM analysis testing the intercept showed that the average similarity between functional connectivity matrices during resting state and the dot-probe task was significantly different than zero across participants, with an average *r*-to-*z* = 0.37, test statistic $t = 20.67$, $p_{FWER} < 0.001$, two-tailed. After controlling for all designs tested, the main PALM analysis with five designs showed that similarity between resting state and the dot-probe task was not related to threat bias, IQ, anxiety symptoms, or social reticence (Table 4). However, when we did not correct for multiple testing, similarity between resting state and the dot-probe task was positively related to threat bias, partial $r = 0.32$, $p_{uncorrected} = 0.03$, $p_{FWER} = 0.23$ (corrected for age, sex, participant recruitment source, and time between scans)[4,5]. This demonstrates that enhanced reconfiguration efficiency relates to greater bias towards threat in children. We calculated the characteristic path length (Rubinov & Sporns, 2010) for both resting state and the dot-probe task, to test whether this effect was driven by differences in rest or task functional connectivity. The relation between threat bias and characteristic path length during both rest and task was not significant, respectively $r = 0.27$, $p = 0.093$ and $r = 0.27$, $p = 0.087$. This suggests that the relation between threat bias and reconfiguration efficiency was not driven by either resting state or the dot-probe task, but rather a combination. The exploratory PALM analysis with twelve designs showed no additional significant effects (see Supplementary Table 2). Finally, to test whether one of the clusters drove the association between similarity and threat bias, we

[4] There was no difference in similarity between resting state and the dot-probe task between participants who did the scans on the same day versus different days, $F(1, 39) = 0.52$, $p = 0.48$. Furthermore, there was no correlation between similarity and the number of days between scans, $r = 0.06$, $p = 0.69$. We repeated the analyses including only children who performed both scans on the same day ($n = 25$). The correlation between similarity and threat bias retained the same direction but was no longer significant, potentially due to lower power, $r = 0.20$, $t = 1.20$, $p_{FWER} = 0.76$, $p_{uncorrected} = 0.12$.

[5] When analyses were repeated with the thresholded (0.5) MELODIC output with the left and right amygdala added to the functional connectivity matrices, the correlation between similarity and threat bias did not remain significant.

calculated similarity between resting state and the dot-probe task for each cluster separately (excluding components 3 and 15 because they belonged to different clusters in rest versus task data). The relation between similarity and threat bias was not significant within each of these clusters, suggesting that the observed correlation is not driven by any of these three clusters, and therefore, may reflect global reconfiguration.

Table 4.

Results of the main PALM analysis with five designs testing the effect of threat bias, IQ, anxiety symptoms and social reticence on similarity between resting state and the dot-probe task.

Independent variable of interest	Contrast	partial *r*	*t*	p_{FWER}
Threat bias	Positive	0.32	2.02	0.23
	Negative	-0.32	-2.02	1.00
IQ	Positive	0.00	-0.02	1.00
	Negative	0.00	0.02	1.00
SCARED-C Total	Positive	-0.19	-1.16	1.00
	Negative	0.19	1.16	0.78
SCARED-P Total	Positive	0.01	0.06	1.00
	Negative	-0.01	-0.06	1.00
Social Reticence	Positive	0.13	0.75	0.96
	Negative	-0.13	-0.75	1.00

Note: *r*s are corrected for the nuisance variables in the design (age, sex, participant recruitment source, and time between scans).

Journal Pre-proof

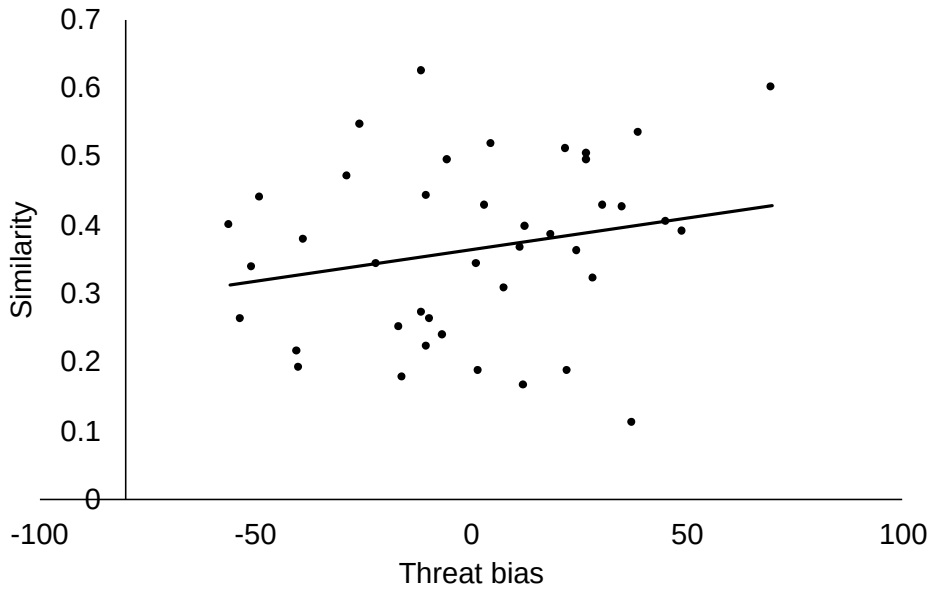

Figure 5. Effect of similarity between resting state and dot-probe task on threat bias.

3.3 PPI analyses

The functional connectivity matrices based on PPI analyses are shown in Figure 6 and 7 (displaying z-statistics, and see Supplementary Figures 3 and 4 for the PPI matrices with *r*s). No significant clusters emerged from the data in either the threat-congruent or threat-incongruent conditions. The first PALM analysis testing the intercept showed that the average similarity between functional connectivity matrices as modulated by threat-congruent and threat-incongruent conditions was significantly different than zero across participants, with an average *r*-to-*z* = −0.11, test statistic $t = -5.28$, $p_{FWER} < 0.001$, two-tailed. The degree to which functional connectivity among brain regions was modulated by the task effects was not related to threat bias, IQ, anxiety symptoms, social reticence, or any other measures from exploratory analyses. The main PALM analysis with five designs showed that the similarity of task-related connectivity modulation between the threat-congruent and threat-incongruent conditions was

unrelated to threat bias, IQ, anxiety symptoms, and social reticence (Table 5). The exploratory PALM analysis with twelve designs showed no additional significant effects (see Supplementary table 3).

Table 5.

Results of the main PALM analysis with five designs testing the effect of threat bias, IQ, anxiety symptoms and social reticence on similarity of modulation by task-related connectivity in threat-congruent and threat-incongruent trials.

Independent variable of interest	Contrast	partial *r*	*t*	p_{FWER}
Threat bias	Positive	-0.15	-0.90	1.00
	Negative	0.15	0.90	0.91
IQ	Positive	-0.03	-0.15	1.00
	Negative	0.03	0.15	1.00
SCARED-C Total	Positive	0.07	0.43	1.00
	Negative	-0.07	-0.43	1.00
SCARED-P Total	Positive	0.01	0.05	1.00
	Negative	-0.01	-0.05	1.00
Social Reticence	Positive	-0.24	-1.46	1.00
	Negative	0.24	1.46	0.56

Note: *r*s are corrected for the nuisance variables in the design (age, sex, participant recruitment source, and time between scans).

Journal Pre-proof

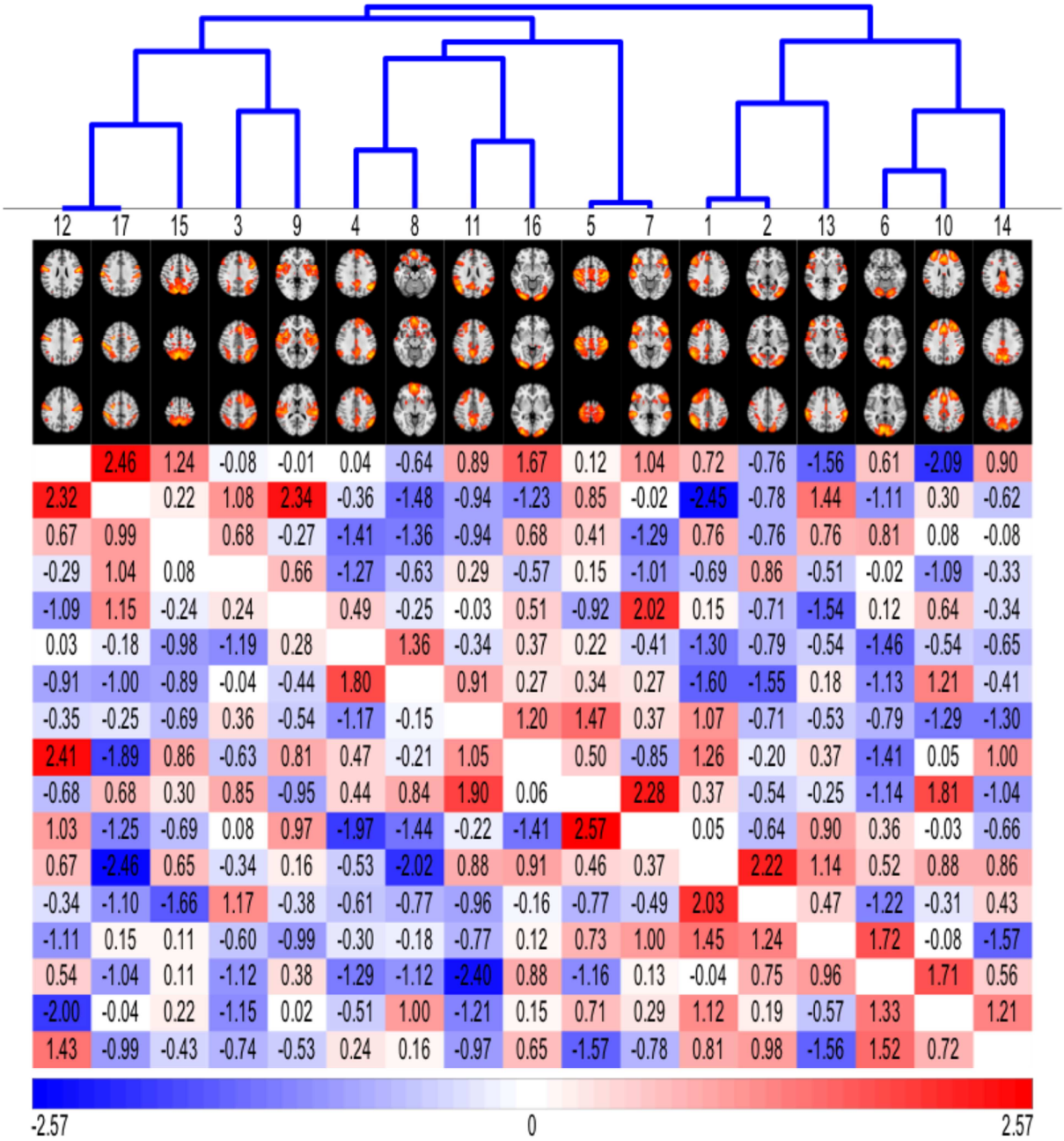

Figure 6. Functional connectivity matrix (transformed to z-statistics) with results from PPI analyses focusing on threat-congruent trials. Components with more similar time courses appear closer together. The threshold for unique colors in the dendrogram was set at 0.75.

Note: numbers correspond to the 17 components (based on resting state data) from Figure 2.

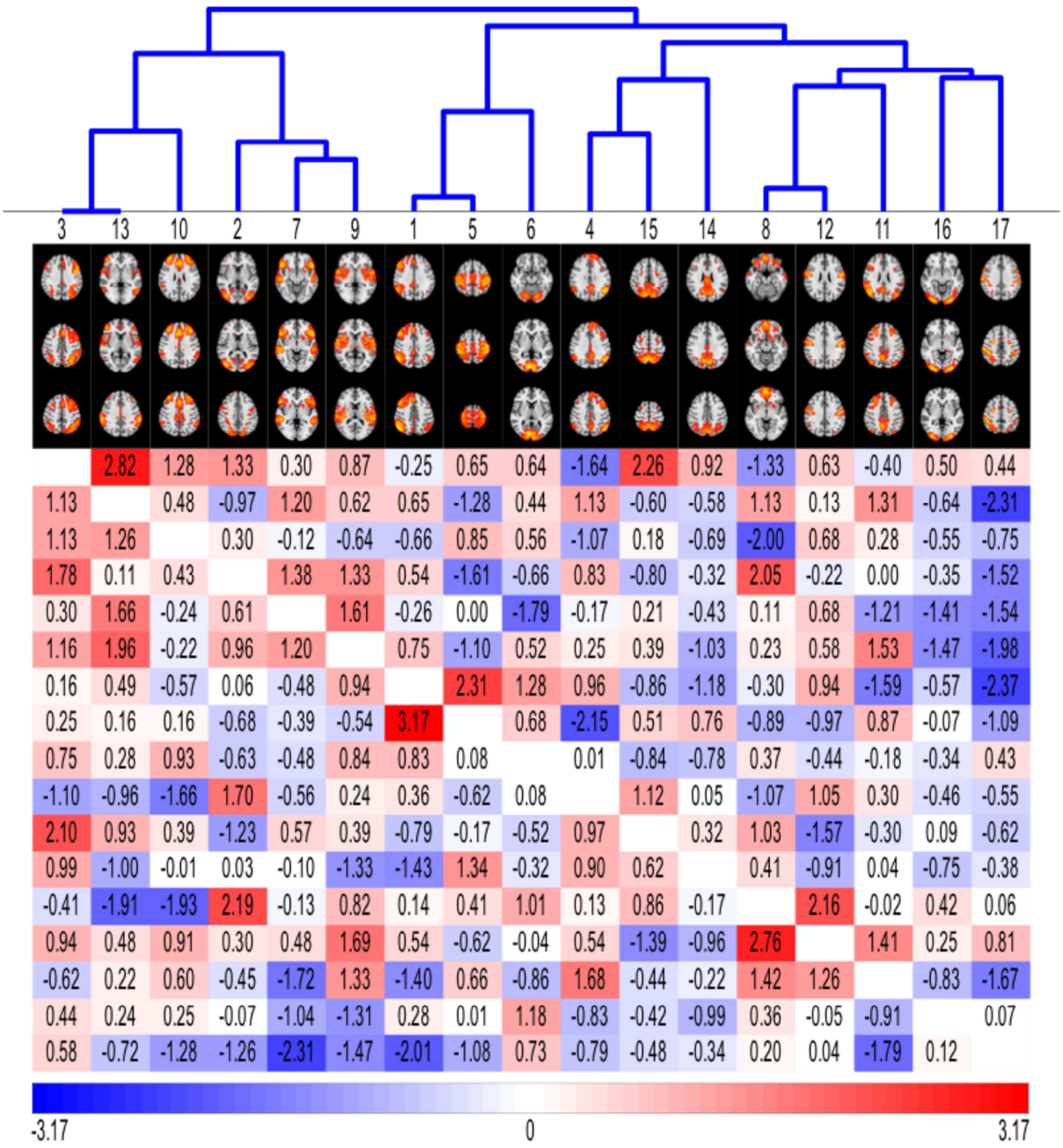

Figure 7. Functional connectivity matrix (transformed to z-statistics) with results from PPI analyses focusing on threat-incongruent trials. Components with more similar time courses appear closer together. The threshold for unique colors in the dendrogram was set at 0.75.

Note: numbers correspond to the 17 components (based on resting state data) from Figure 2.

Journal Pre-proof

4. Discussion

The goal of the current study was to examine whether similarity in functional connectivity during rest and the dot-probe task relates to threat bias, IQ, anxiety symptoms and social reticence in children. The study generated three main findings. First, functional connectivity during rest and dot-probe was positively correlated. Second, levels of similarity between rest and the dot-probe task related to threat bias, but not to IQ, anxiety symptoms or socially reticent behavior. However, this finding should be interpreted with caution since the association did not remain significant when correcting for all tested designs. Finally, functional connectivity based on PPI analyses was negatively correlated between threat-congruent and threat-incongruent conditions, though such task-related modulation in connectivity did not relate to measures of threat bias nor anxiety.

Functional connectivity during rest and the dot-probe task was positively correlated, suggesting that functional hierarchies in the brain are stable (Cole et al., 2014; Smith et al., 2009). Our finding extends similar findings from previous studies focusing on cognitive tasks in adults (Cole et al., 2014; Schultz & Cole, 2016; Smith et al., 2009) to an emotional task in children. In addition, we have shown that these functional hierarchies in the brain can also be found using a resting-state ICA approach which has not been used in previous studies.

Similarity in functional connectivity during rest and the dot-probe task was positively related to threat bias, although this did not survive correction for multiple testing. This pattern of findings suggests that children with a greater bias towards threat possess greater efficiency in switching from resting state to the dot-probe task. This might further imply that, in children with threat bias, the brain during rest could already be preconfigured to a threat-bias state. This could be related to anxiety symptoms, as threat-related attentional biases are related to anxiety (Bar-

Haim et al., 2007). Approximately half of the participants were drawn from infants selected for heightened risk for psychopathology, but this greater efficiency in switching from resting state to a threat-bias state was not related to anxiety. However, the participants were relatively young and had few anxiety symptoms, which typically increase in mid-adolescence. Future studies examining children with anxiety disorders are needed to clarify if children with anxiety disorders are more preconfigured to a threat-bias state and the clinical implications of these findings.

The current study demonstrates comparable effects, in terms of correlations between similarity and task performance, for an emotional task to the effects for cognitive tasks used in prior research. Importantly, in the current study, the correlation between reconfiguration efficiency and attention bias would be classified as a small-to-medium effect size, using criteria from J. Cohen (1988), and was only significant before correction for multiple testing. Similarly, Schultz and Cole (2016) detected associations between reconfiguration efficiency and measures of task performance across three cognitive tasks that also would be classified as small-to-medium. The current focus on an emotional instead of cognitive tasks may explain other differences in the observed findings between the current study and Schultz and Cole (2016). For example, Schultz and Cole (2016) related reconfiguration efficiency for cognitive tasks to both performance on cognitive tasks and IQ, the two of which were correlated (Schultz & Cole, 2016). In the current study, threat bias during the dot-probe task was not related to IQ ($r = 0.13$, $p = 0.43$), possibly explaining why there was no correlation between reconfiguration efficiency and IQ in the current study.

Variations in brain parcellations, such as anatomical templates or ICA-based functional networks, can influence the number of statistical tests performed in a study (Eickhoff, Yeo, & Genon, 2018). We did not use the same approach as Schultz and Cole (2016) because they used a

Journal Pre-proof

template derived from data in adults (Power et al., 2011). In addition, a paucity of time points in our data precluded partial correlation computations for 264 regions. For these reasons we performed an ICA on the resting state data to reduce the data to 17 networks. Beyond reducing the number of parameters, ICA has other key advantages: it reliably identifies resting state networks that are interpretable (Damoiseaux et al., 2006), that resemble discrete functional units (Beckmann et al., 2005), that have spatial correspondence with task-related activity (Smith et al., 2009), and that are heritable (Glahn et al., 2010). Group ICA, as was used here, captures spatial patterns that are consistent across participants, being less prone to subject-specific variability or artefacts than other methods. Of note, our results for threat bias associations were non-significant when applying another parcellation (Yeo et al., 2011) complemented with additional, subcortical regions derived from FreeSurfer.

A final set of unique observations arose from the PPI analyses. These analyses showed that levels of event-related modulation of functional connectivity were negatively correlated for the threat-congruent and threat-incongruent trials. These two trial types represent events where the spatial location of threats and probes lie in respectively similar and opposite hemi-fields. Such negative correlations could arise from the unique psychological demands placed on children from distinct event types, i.e. maintaining versus redirecting attention. Both previous studies and our current findings reveal positive correlations between functional connectivity during rest and tasks, suggesting that task-related connectivity consists of both intrinsic, task-general, and task-specific network activity (Cole et al., 2014). The negative correlation between threat-congruent and threat-incongruent could be interpreted as reflecting the deployment of task-specific changes in network connectivity, related to the distinct attentional demands of the threat-congruent and threat-incongruent trials. By examining these task-specific changes, the

current study adds to the repertoire of available tools for understanding the potential clinical significance of individual differences in functional connectivity.

This study showed that similarity in functional connectivity during rest and the dot-probe task was related to threat bias in children (although, as noted, this correlation did not survive correction for multiple testing), extending previous research on cognitive tasks in adults to an emotional task in children. Several limitations should be noted, however. First, the sample size was relatively small. Second, the sample consisted of mostly typically developing children, only half of whom were selected for risk for anxiety, thus there may have been insufficient variability to precisely estimate associations with anxiety symptoms. In addition, some participants completed the SCARED up to a year apart from the MRI scans. Although the SCARED has shown acceptable test-retest reliability (Behrens et al., 2019; Birmaher et al., 1997; Boyd et al., 2003; Haley et al., 2011), these estimates of test-retest reliability mainly arise in studies using time windows that do not extend beyond six months. Future research in larger samples of anxious patients with concurrent assessment of symptoms is needed to test if similarity in functional connectivity during rest and the dot-probe task is related to anxiety symptoms. Third, fMRI during resting state and the dot-probe task was not measured on the same day in all children. Even though resting state functional networks have high reproducibility over 3.5 years, some changes can be seen over time (Choe et al., 2015; Poldrack et al., 2015). Therefore, future research should attempt to collect resting state and task data on the same day. We did find a positive correlation between functional connectivity during rest and task, so future studies should indicate if this similarity could be seen as a trait measure or how it develops over time. Fourth, we used a canonical HRF approach to regress out task activations instead of a finite impulse response (FIR) task regression. A recent paper (Cole et al., 2019) has shown that task FC

Journal Pre-proof

estimates may be consistently and spuriously influenced by task activations, and that the FIR approach is the best way to correct for this. We were not able to apply this FIR approach because we would not have had enough degrees of freedom for the analysis. Future studies should consider the possibility of FIR modelling for the removal of task effects.

To conclude, functional connectivity during rest and the dot-probe task was positively correlated, confirming previous findings of stable functional hierarchies in the brain. Reconfiguration efficiency was related to threat bias if we did not correct for multiple testing. Children with a bias towards threat might be more prone to process threat, as they can more efficiently switch from rest to threat processing. Modulation of functional connectivity by task-evoked activity during threat-congruent and threat-incongruent trials was negatively correlated, possibly reflecting task-specific network changes during two different attentional processes. We applied a novel analytic method for combining resting state and task-related fMRI data to an emotional paradigm in children. The next step in applying this method in the field of developmental psychopathology would be to test between-group differences in a larger sample of children with and without anxiety disorders.

Journal Pre-proof

Journal Pre-proof

Acknowledgements

This work was supported by the National Institute of Mental Health (R37HD17899 and U01MH093349) and the Intramural Research Program at the National Institute of Mental Health (ZIA-MH-002782 and NCT00018057).

Declarations of interest: none

Journal Pre-proof

Journal Pre-proof

References

Abend, R., de Voogd, L., Salemink, E., Wiers, R. W., Perez-Edgar, K., Fitzgerald, A., . . . Bar-Haim, Y. (2018). Association between attention bias to threat and anxiety symptoms in children and adolescents. *Depression and Anxiety, 35*(3), 229-238. doi:10.1002/da.22706

Abend, R., Swetlitz, C., White, L. K., Shechner, T., Bar-Haim, Y., Filippi, C., . . . Pine, D. S. (2019). Levels of early-childhood behavioral inhibition predict distinct neurodevelopmental pathways to pediatric anxiety. *Psychological Medicine*, 1-11. doi:10.1017/S0033291718003999

Bar-Haim, Y., Lamy, D., Pergamin, L., Bakermans-Kranenburg, M. J., & van IJzendoorn, M. H. (2007). Threat-related attentional bias in anxious and nonanxious individuals: A meta-analytic study. *Psychological Bulletin, 133*(1), 1-24. doi:10.1037/0033-2909.133.1.1

Beckmann, C. F., DeLuca, M., Devlin, J. T., & Smith, S. M. (2005). Investigations into resting-state connectivity using independent component analysis. *Philosophical Transactions of the Royal Society B-Biological Sciences, 360*(1457), 1001-1013. doi:10.1098/rstb.2005.1634

Beckmann, C. F., & Smith, S. A. (2004). Probabilistic independent component analysis for functional magnetic resonance imaging. *Ieee Transactions on Medical Imaging, 23*(2), 137-152. doi:10.1109/tmi.2003.822821

Behrens, B., Swetlitz, C., Pine, D. S., & Pagliaccio, D. (2019). The Screen for Child Anxiety Related Emotional Disorders (SCARED): Informant discrepancy, measurement Iivariance, and test-retest reliability. *Child Psychiatry & Human Development, 50*(3), 473-482. doi:10.1007/s10578-018-0854-0

Behzadi, Y., Restom, K., Liau, J., & Liu, T. T. (2007). A component based noise correction method (CompCor) for BOLD and perfusion based fMRI. *Neuroimage, 37*(1), 90-101. doi:10.1016/j.neuroimage.2007.04.042

Birmaher, B., Khetarpal, S., Brent, D., Cully, M., Balach, L., Kaufman, J., & Neer, S. M. (1997). The screen for child anxiety related emotional disorders (SCARED): Scale construction and psychometric characteristics. *Journal of the American Academy of Child and Adolescent Psychiatry, 36*(4), 545-553. doi:10.1097/00004583-199704000-00018

Bolt, T., Nomi, J. S., Rubinov, M., & Uddin, L. Q. (2017). Correspondence between evoked and intrinsic functional brain network configurations. *Human Brain Mapping, 38*(4), 1992-2007. doi:10.1002/hbm.23500

Boyd, R. C., Ginsburg, G. S., Lambert, S. F., Cooley, M. R., & Campbell, K. D. M. (2003). Screen for Child Anxiety Related Emotional Disorders (SCARED): Psychometric properties in an African-American parochial high school sample. *Journal of the American Academy of Child and Adolescent Psychiatry, 42*(10), 1188-1196. doi:10.1097/01.chi.0000082033.88099.8d

Bruhl, A. B., Delsignore, A., Komossa, K., & Weidt, S. (2014). Neuroimaging in social anxiety disorder - A meta-analytic review resulting in a new neurofunctional model. *Neuroscience and Biobehavioral Reviews, 47*, 260-280. doi:10.1016/j.neubiorev.2014.08.003

Canivez, G. L., & Watkins, M. W. (1998). Long-term stability of the Wechsler intelligence scale for Children - Third edition. *Psychological Assessment, 10*(3), 285-291. doi:10.1037/1040-3590.10.3.285

Choe, A. S., Jones, C. K., Joel, S. E., Muschelli, J., Belegu, V., Caffo, B. S., . . . Pekar, J. J. (2015). Reproducibility and temporal structure in weekly resting-state fMRI over a period of 3.5 years. *Plos One, 10*(10). doi:10.1371/journal.pone.0140134

Cohen, J. (1988). *Statistical power analysis for the behavioral sciences*: Routledge.

Cohen, J. R., & D'Esposito, M. (2016). The segregation and integration of distinct brain networks and their relationship to cognition. *Journal of Neuroscience, 36*(48), 12083-12094. doi:10.1523/jneurosci.2965-15.2016

Cole, M. W., Bassett, D. S., Power, J. D., Braver, T. S., & Petersen, S. E. (2014). Intrinsic and task-evoked network architectures of the human brain. *Neuron, 83*(1), 238-251. doi:10.1016/j.neuron.2014.05.014

Cole, M. W., Ito, T., Schultz, D., Mill, R., Chen, R., & Cocuzza, C. (2019). Task activations produce spurious but systematic inflation of task functional connectivity estimates. *Neuroimage, 189*, 1-18. doi:10.1016/j.neuroimage.2018.12.054

Damoiseaux, J. S., Rombouts, S. A. R. B., Barkhof, F., Scheltens, P., Stam, C. J., Smith, S. M., & Beckmann, C. F. (2006). Consistent resting-state networks across healthy subjects. *Proceedings of the National Academy of Sciences of the United States of America, 103*(37), 13848-13853. doi:10.1073/pnas.0601417103

de Lijster, J. M., Dierckx, B., Utens, E., Verhulst, F. C., Zieldorff, C., Dieleman, G. C., & Legerstee, J. S. (2017). The age of onset of anxiety disorders: A meta-analysis. *Canadian Journal of Psychiatry-Revue Canadienne De Psychiatrie, 62*(4), 237-246. doi:10.1177/0706743716640757

Degnan, K. A., Almas, A. N., Henderson, H. A., Hane, A. A., Walker, O. L., & Fox, N. A. (2014). Longitudinal trajectories of social reticence with unfamiliar peers across early childhood. *Developmental Psychology, 50*(10), 2311-2323. doi:10.1037/a0037751

Degnan, K. A., Hane, A. A., Henderson, H. A., Moas, O. L., Reeb-Sutherland, B. C., & Fox, N. A. (2011). Longitudinal stability of temperamental exuberance and social-emotional outcomes in early childhood. *Developmental Psychology*, *47*(3), 765-780. doi:10.1037/a0021316

Eickhoff, S. B., Yeo, B. T. T., & Genon, S. (2018). Imaging-based parcellations of the human brain. *Nature Reviews Neuroscience, 19*(11), 672-686. doi:10.1038/s41583-018-0071-7

Esteban, O., Birman, D., Schaer, M., Koyejo, O. O., Poldrack, R. A., & Gorgolewski, K. J. (2017). MRIQC: Advancing the automatic prediction of image quality in MRI from unseen sites. *Plos One, 12*(9). doi:10.1371/journal.pone.0184661

Esteban, O., Markiewicz, C. J., Blair, R. W., Moodie, C. A., Isik, A. I., Erramuzpe, A., . . . Gorgolewski, K. J. (2019). fMRIPrep: a robust preprocessing pipeline for functional MRI. *Nature Methods, 16*(1), 111-116. doi:10.1038/s41592-018-0235-4

Etkin, A., & Wager, T. D. (2007). Functional neuroimaging of anxiety: A meta-analysis of emotional processing in PTSD, social anxiety disorder, and specific phobia. *American Journal of Psychiatry, 164*(10), 1476-1488. doi:10.1176/appi.ajp.2007.07030504

Filippini, N., MacIntosh, B. J., Hough, M. G., Goodwin, G. M., Frisoni, G. B., Smith, S. M., . . . Mackay, C. E. (2009). Distinct patterns of brain activity in young carriers of the APOE-epsilon 4 allele. *Proceedings of the National Academy of Sciences of the United States of America, 106*(17), 7209-7214. doi:10.1073/pnas.0811879106

Fox, M. D., & Raichle, M. E. (2007). Spontaneous fluctuations in brain activity observed with functional magnetic resonance imaging. *Nature Reviews Neuroscience, 8*(9), 700-711. doi:10.1038/nrn2201

Friston, K. J., Buechel, C., Fink, G. R., Morris, J., Rolls, E., & Dolan, R. J. (1997). Psychophysiological and modulatory interactions in neuroimaging. *Neuroimage, 6*(3), 218-229. doi:10.1006/nimg.1997.0291

Glahn, D. C., Winkler, A. M., Kochunov, P., Almasy, L., Duggirala, R., Carless, M. A., . . . Blangero, J. (2010). Genetic control over the resting brain. *Proceedings of the National Academy of Sciences of the United States of America, 107*(3), 1223-1228. doi:10.1073/pnas.0909969107

Glover, G. H. (1999). Deconvolution of impulse response in event-related BOLD fMRI. *Neuroimage, 9*(4), 416-429. doi:10.1006/nimg.1998.0419

Goldsmith, H. H. (1996). Studying temperament via construction of the toddler behavior assessment questionnaire. *Child Development, 67*(1), 218-235. doi:10.2307/1131697

Hale, W. W., Raaijmakers, Q., Muris, P., van Hoof, A., & Meeus, W. (2008). Developmental trajectories of adolescent anxiety disorder symptoms: A 5-year prospective community study. *Journal of the American Academy of Child and Adolescent Psychiatry, 47*(5), 556-564. doi:10.1097/CHI.0b013e3181676583

Haley, T., Puskar, K., & Terhorst, L. (2011). Psychometric properties of the Screen for Child Anxiety Related Emotional Disorders in a rural high school population. *Journal of Child and Adolescent Psychiatric Nursing, 24*(1), 23-32. doi:10.1111/j.1744-6171.2010.00264.x

Hane, A. A., Fox, N. A., Henderson, H. A., & Marshall, P. J. (2008). Behavioral reactivity and approach-withdrawal bias in infancy. *Developmental Psychology, 44*(5), 1491-1496. doi:10.1037/a0012855

Hardee, J. E., Benson, B. E., Bar-Haim, Y., Mogg, K., Bradley, B. P., Chen, G., . . . Perez-Edgar, K. (2013). Patterns of neural connectivity during an attention bias task moderate associations between early childhood temperament and internalizing symptoms in young adulthood. *Biological Psychiatry, 74*(4), 273-279. doi:10.1016/j.biopsych.2013.01.036

Hearne, L. J., Cocchi, L., Zalesky, A., & Mattingley, J. B. (2017). Reconfiguration of brain network architectures between resting-state and complexity-dependent cognitive reasoning. *Journal of Neuroscience, 37*(35), 8399-8411. doi:10.1523/jneurosci.0485-17.2017

Iacoviello, B. M., Wu, G., Abend, R., Murrough, J. W., Feder, A., Fruchter, E., . . . Charney, D. S. (2014). Attention bias variability and symptoms of posttraumatic stress disorder. *Journal of Traumatic Stress, 27*(2), 232-239. doi:10.1002/jts.21899

Ito, T., Kulkarni, K. R., Schultz, D. H., Mill, R. D., Chen, R. H., Solomyak, L. I., & Cole, M. W. (2017). Cognitive task information is transferred between brain regions via resting-state network topology. *Nature Communications, 8*(1027). doi:10.1038/s41467-017-01000-w

Jarcho, J. M., Davis, M. M., Shechner, T., Degnan, K. A., Henderson, H. A., Stoddard, J., . . . Nelson, E. E. (2016). Early-childhood social reticence predicts brain function in preadolescent youths during distinct forms of peer evaluation. *Psychological Science, 27*(6), 821-835. doi:10.1177/0956797616638319

Macleod, C., Mathews, A., & Tata, P. (1986). Attentional bias in emotional disorders. *Journal of Abnormal Psychology, 95*(1), 15-20. doi:10.1037/0021-843x.95.1.15

Mennes, M., Kelly, C., Zuo, X. N., Di Martino, A., Biswal, B. B., Castellanos, F. X., & Milham, M. P. (2010). Inter-individual differences in resting-state functional connectivity predict task-induced BOLD activity. *Neuroimage, 50*(4), 1690-1701. doi:10.1016/j.neuroimage.2010.01.002

Michalska, K. J., Feldman, J. S., Ivie, E. J., Shechner, T., Sequeira, S., Averbeck, B., . . . Pine, D. S. (2019). Early-childhood social reticence predicts SCR-BOLD coupling during fear extinction recall in preadolescent youth. *Developmental Cognitive Neuroscience, 39*(100605). doi:10.1016/j.dcn.2018.12.003

Muris, P., Dreessen, L., Bogels, S., Weckx, M., & van Melick, M. (2004). A questionnaire for screening a broad range of DSM-defined anxiety disorder symptoms in clinically referred children and adolescents. *Journal of Child Psychology and Psychiatry, 45*(4), 813-820. doi:10.1111/j.1469-7610.2004.00274.x

O'Reilly, J. X., Woolrich, M. W., Behrens, T. E. J., Smith, S. M., & Johansen-Berg, H. (2012). Tools of the trade: psychophysiological interactions and functional connectivity. *Social Cognitive and Affective Neuroscience, 7*(5), 604-609. doi:10.1093/scan/nss055

Poldrack, R. A., Laumann, T. O., Koyejo, O., Gregory, B., Hover, A., Chen, M. Y., . . . Mumford, J. A. (2015). Long-term neural and physiological phenotyping of a single human. *Nature Communications, 6*, 15. doi:10.1038/ncomms9885

Power, J. D., Barnes, K. A., Snyder, A. Z., Schlaggar, B. L., & Petersen, S. E. (2012). Spurious but systematic correlations in functional connectivity MRI networks arise from subject motion. *Neuroimage, 59*(3), 2142-2154. doi:10.1016/j.neuroimage.2011.10.018

Journal Pre-proof

Power, J. D., Cohen, A. L., Nelson, S. M., Wig, G. S., Barnes, K. A., Church, J. A., . . . Petersen, S. E. (2011). Functional network organization of the human brain. *Neuron, 72*(4), 665-678. doi:10.1016/j.neuron.2011.09.006

Pruim, R. H. R., Mennes, M., van Rooij, D., Llera, A., Buitelaar, J. K., & Beckmann, C. F. (2015). ICA-AROMA: A robust ICA-based strategy for removing motion artifacts from fMRI data. *Neuroimage, 112*, 267-277. doi:10.1016/j.neuroimage.2015.02.064

Rothbart, M. K., Ahadi, S. A., Hershey, K. L., & Fisher, P. (2001). Investigations of temperament at three to seven years: The children's behavior questionnaire. *Child Development, 72*(5), 1394-1408. doi:10.1111/1467-8624.00355

Rubinov, M., & Sporns, O. (2010). Complex network measures of brain connectivity: Uses and interpretations. *Neuroimage, 52*(3), 1059-1069. doi:10.1016/j.neuroimage.2009.10.003

Schultz, D. H., & Cole, M. W. (2016). Higher intelligence is associated with less task-related brain network reconfiguration. *Journal of Neuroscience, 36*(33), 8551-8561. doi:10.1523/jneurosci.0358-16.2016

Smith, S. M., Fox, P. T., Miller, K. L., Glahn, D. C., Fox, P. M., Mackay, C. E., . . . Beckmann, C. F. (2009). Correspondence of the brain's functional architecture during activation and rest. *Proceedings of the National Academy of Sciences of the United States of America, 106*(31), 13040-13045. doi:10.1073/pnas.0905267106

Smith, S. M., Vidaurre, D., Beckmann, C. F., Glasser, M. F., Jenkinson, M., Miller, K. L., . . . Van Essen, D. C. (2013). Functional connectomics from resting-state fMRI. *Trends in Cognitive Sciences, 17*(12), 666-682. doi:10.1016/j.tics.2013.09.016

Journal Pre-proof

Tottenham, N., Tanaka, J. W., Leon, A. C., McCarry, T., Nurse, M., Hare, T. A., . . . Nelson, C. (2009). The NimStim set of facial expressions: Judgments from untrained research participants. *Psychiatry Research, 168*(3), 242-249. doi:10.1016/j.psychres.2008.05.006

Watkins, M. W., & Smith, L. G. (2013). Long-term stability of the Wechsler Intelligence Scale for Children-Fourth Edition. *Psychological Assessment, 25*(2), 477-483. doi:10.1037/a0031653

Wechsler, D. (1999). *Wechsler Abbreviated Scale of Intelligence*. San Antonio, TX: The Psychological Corporation.

White, L. K., Britton, J. C., Sequeira, S., Ronkin, E. G., Chen, G., Bar-Haim, Y., . . . Pine, D. S. (2016). Behavioral and neural stability of attention bias to threat in healthy adolescents. *Neuroimage, 136*, 84-93. doi:10.1016/j.neuroimage.2016.04.058

White, L. K., Sequeira, S., Britton, J. C., Brotman, M. A., Gold, A. L., Berman, E., . . . Pine, D. S. (2017). Complementary features of attention bias modification therapy and cognitive-behavioral therapy in pediatric anxiety disorders. *American Journal of Psychiatry, 174*(8), 775-784. doi:10.1176/appi.ajp.2017.16070847

Winkler, A. M., Ridgway, G. R., Webster, M. A., Smith, S. M., & Nichols, T. E. (2014). Permutation inference for the general linear model. *Neuroimage, 92*, 381-397. doi:10.1016/j.neuroimage.2014.01.060

Winkler, A. M., Webster, M. A., Brooks, J. C., Tracey, I., Smith, S. M., & Nichols, T. E. (2016). Non-parametric combination and related permutation tests for neuroimaging. *Human Brain Mapping, 37*(4), 1486-1511. doi:10.1002/hbm.23115

Xu, J., Van Dam, N. T., Feng, C. L., Luo, Y. J., Ai, H., Gu, R. L., & Xu, P. F. (2019). Anxious brain networks: A coordinate-based activation likelihood estimation meta-analysis of

resting-state functional connectivity studies in anxiety. *Neuroscience and Biobehavioral Reviews, 96*, 21-30. doi:10.1016/j.neubiorev.2018.11.005

Yeo, B. T. T., Krienen, F. M., Sepulcre, J., Sabuncu, M. R., Lashkari, D., Hollinshead, M., . . . Buckner, R. L. (2011). The organization of the human cerebral cortex estimated by intrinsic functional connectivity. *Journal of Neurophysiology, 106*(3), 1125-1165. doi:10.1152/jn.00338.2011

Journal Pre-proof